THE ASTROPHYSICAL JOURNAL, 231:277–283, 1979 July 1

PARTIAL REDISTRIBUTION IN THE SOLAR PHOTOSPHERIC Ba II SPECTRUM

ROBERT J. RUTTEN†
Sacramento Peak Observatory*
AND
ROBERT W. MILKEY
Kitt Peak National Observatory*
Received 1978 December 8; accepted 1979 January 19

ABSTRACT

We extend recent studies of the effects of partial frequency redistribution (PRD) on the formation of strong chromospheric resonance lines to weaker lines formed in the photosphere. Methods that have been derived to compute the PRD formation of the Ca II spectrum are applied to the solar Ba II spectrum. We find that PRD is important in the formation of the λ4554 resonance line, and we confirm that its effects on the line source function explain the emission wings of this line observed near the limb. Source function structure and line profiles for Ba II λ4554 and Ba II λ5854 are discussed; they may serve as an example for estimating effects of PRD in other photospheric lines in stellar atmospheres.

Subject headings: line formation — radiative transfer — Sun: atmosphere — Sun: spectra

I. INTRODUCTION

The effects of partial frequency redistribution (PRD) have been found to be quite important in various strong chromospheric resonance lines (e.g., Lα: Vernazza, Avrett, and Loeser 1973; Milkey and Mihalas 1973*a*, *b*; Mg II h and k: Milkey and Mihalas 1974; Ca II H and K: Vardavas and Cram 1974; Shine, Milkey, and Mihalas 1975; Mg I λ2852: Canfield and Cram 1977. A review of PRD in the astrophysical context has been given by Milkey 1976). All of these lines are very strong, so that their inner wings, outside the Doppler-redistributed cores (Thomas 1957), are formed at heights where radiative damping ($\gamma_{\rm rad}$) greatly exceeds collisional damping ($\gamma_{\rm coll}$). In these inner wings, collisional damping will only slightly destroy the coherence of the scattering process.

In this paper, we study the importance of PRD effects for a *weaker* photospheric resonance line. For very weak lines, the assumption of complete redistribution (CRD) will be valid because the entire line wings will be formed in deep layers where collisions effectively destroy coherence. The question is how weak the line has to be.

A good candidate for such a study is the Ba II resonance line at 4554 Å (e.g., Underhill 1973). The level structure of the Ba II ion is similar to that of the Ca II ion, but the λ4554 resonance line is much weaker than the corresponding Ca II K line because of the calcium/barium abundance ratio of 10^4.

In a previous study (Rutten 1978, hereafter Paper I), the effects of PRD on the formation of λ4554 were found to be only slight on the disk, but pronounced at the extreme limb. PRD effects increase toward the limb because the extent in wavelength of the coherently scattered inner wings increases. The outer CRD–PRD changeover in the profile is approximately at that wavelength separation from line center for which the line radiation originates at the height where $\gamma_{\rm rad} = \gamma_{\rm coll}$; toward the limb, the radiation at a given wavelength comes from progressively higher layers, and the CRD–PRD changeover shifts outward in the profile. At the same time, the width of the Doppler-redistributed core, which sets the location in the profile of the inner PRD–CRD changeover, decreases toward the limb because both the thermal and nonthermal components of the Doppler width decrease with height.

In Paper I, it was assumed that these effects were large enough in λ4554 to uncouple the monochromatic source function in the line wings from the line core source function. This independence of the wing source function was then employed to explain the emission wings that the λ4554 line displays near the solar limb as being due to the wing source function's following the monochromatic mean intensity J_ν outward and rising above the local Planck function. The limb emission wings of λ4554 were thus attributed to a scattering-dominated, weak-line source function, similar to Canfield's (1969, 1971) Ca II limb emission lines.

In the analysis of Paper I, the λ4554 frequency-dependent line source function and other Ba II line formation parameters were inferred empirically by a trial-and-error profile fitting process. Since the results are not unique (as for any line-profile synthesis

* Operated by the Association of Universities for Research in Astronomy, Inc., under contract with the National Science Foundation.

† On leave from The Astronomical Institute, Sterrewacht "Sonnenborgh," Utrecht, The Netherlands.

study), it is of interest to solve the non–LTE radiative transfer equations for the line source functions of the Ba II lines in a numerical model-atom computation, including PRD. We use the methods derived by Milkey, Shine, and Mihalas (1975) for the Ca II ion. Because we are limited by uncertainties in parameters and also in computing resources, we do not aim for a detailed fit to all observations; rather, we concentrate on demonstrating the differences between CRD and PRD computations. The results may be used to estimate the importance of PRD in the formation of other photospheric lines in stellar atmospheres.

II. CALCULATION OF Ba II PROFILES

a) The Model Atom

We use a four-level atomic model consisting of the $6^2S_{1/2}$ ground level, the $5^2D_{3/2}$ and $5^2D_{5/2}$ metastable levels, and the $6^2P_{3/2}$ level. This is the equivalent to the three-level approximation to the Ca II ion used by Shine *et al.* (1975), but with both ^2D metastable levels included. In Ba II, these levels contribute appreciably to the number conservation equation because their excitation potentials (0.6–0.7 eV) are so low, while in Ca II only the metastable level participating in a radiative transition must be included.

Owing to limited computing capacity, we solve for two lines only. In addition to the λ4554 resonance line ($6P_{3/2}$–$6S_{1/2}$, equivalent width at disk center 188 mÅ), we computed the λ5854 line ($6P_{3/2}$–$5D_{3/2}$, 63 mÅ). This weak line was chosen instead of the stronger λ6142 line ($6P_{3/2}$–$5D_{5/2}$, 120 mÅ) because the latter is blended by Fe λ6141.7 (multiplet 816, 30–40 mÅ). Comparison computations with λ6142 instead of λ5854 show that this replacement does not significantly affect the formation of the λ4554 line. A more complete representation would add the $6^2S_{3/2}$ level and solve for all five lines (λ4554, λ4934; λ5854, λ6142, λ6497). Experience with Ca II (Shine *et al.* 1975) indicates that while the absolute intensities may change by factors of 1.5–2 in the inner wing when the extended model is used, the differential effects between the PRD and CRD solutions will be preserved.

Collision rates for bound-bound transitions were taken from Tandberg-Hanssen and Smythe (1970, Table 4). Collisional ionization rates are computed following Tandberg-Hanssen (1964, eqs. [32] and [35]). Photoionization and radiative recombination rates are taken from Tandberg-Hanssen (1964, Table 10). These are for fixed radiation fields at all depths, and are therefore strictly applicable only where the continuum optical depth is less than unity. However, throughout the line-forming region Ba III is present in such minute quantities that the error is negligible.

The line parameter values (oscillator strengths, natural broadening, and collisional broadening) were taken from Paper I. The collisional broadening values are from the Smirnov-Roueff potential formalism of Deridder and Van Rensbergen (1974) for λ4554, here taken equal in frequency units for λ5854. These are 1.5 times the classical Van der Waals value for λ4554, in agreement with the result of Fullerton and Cowley (1971).

b) The Model Atmosphere

We employed the HSRA (Gingerich *et al.* 1971). Since we discuss eclipse observations, the height scale we use and display in the figures is the eclipse scale, which has its zero at +337 km on the HSRA scale.

The continuum source function is assumed to be in LTE, except for the contribution by electron scattering. The microturbulence, macroturbulence, and barium abundance were adjusted.

c) Computational Techniques

The coupled radiative transfer and statistical equilibrium problem is solved following Milkey *et al.* (1975). This method allows for the existence of the metastable $5D$ levels and both the λ4554 and λ5854 transitions by defining "cross" redistribution processes to account for photons absorbed in one line and re-emitted in the other line. The redistribution matrices R^{II} and R^{X} were also generated following Milkey *et al.* (1975).

The synthesis of the emergent profiles is done with an adaption of the curved-layer program of Paper I. The hyperfine structure of λ4554 is included following Paper I and assuming source function equality in the three components. Since their maximum separation is only about two Doppler widths and they are not resolved in the solar spectrum, this is probably a very good approximation. For comparison with the eclipse observations of λ4554 at the extreme limb (Rutten 1977), we compute line profiles from the proper spherical geometry and take the effects of atmospheric seeing into account (see Paper I).

d) Sensitivity to Line Parameters: Turbulence

Various test computations have been done with different input parameters. The resulting line profiles are not very sensitive to the assumed collisional excitation rates and radiative recombination rates; much more important are the barium abundance, the collisional broadening, and, above all, the microturbulence.

The sensitivity of line profiles to collisional damping and microturbulence is enhanced in PRD computations because these parameters then control the frequency dependence of the line source function. For strong lines, the enhancement of the sensitivity to γ_{Coll} is well known (see Milkey 1976); for the weaker λ4554 line the CRD–to–PRD changeover from Doppler core to coherent inner wing is more important. The problem that arises is to estimate to what extent and how nonthermal motions contribute to the redistribution in the core.

We follow the usual way of accounting for the nonthermal motions and the inhomogeneities in the photosphere with the quantities "microturbulence" and "macroturbulence," which define convolutions with normal distributions, respectively, of the local line absorption coefficient and the emergent profile. The height-dependent microturbulence then represents an addition to the local thermal motions, and we

follow Shine *et al.* (1975) in assuming that it contributes similarly to the Doppler width and the Doppler redistribution in the line core.

However, this is not a rigorous description. Magnan (1975) has pointed out that the redistribution functions will depend on the motions of the scattering atoms; more generally, the micro/macroturbulence formalism itself is questionable. In the quiet photosphere, the observed granular structure, granular motions, five-minute oscillations, and possibly short-period oscillations all represent components of the broadening of spectral lines observed at low spatial resolution. These components appear on macroscale, but may well contribute also to the microturbulence in the usual profile-fitting analyses, in which the "turbulences" are the final adjustment parameters to reproduce the observations. The reason for this is that the microturbulence furnishes many more free parameters, owing to its height-dependence, than the macroturbulence. Obviously, these resolvable components vary substantially with height and with viewing angle (see Keil and Canfield 1978), and more than a single-valued broadening parameter will be needed to describe properly their effects on spatially-averaged line profile observations. We conclude that a detailed discussion of redistribution functions in the presence of nonthermal motions will be worthwhile only after these large-scale contributions have been extracted and the small-scale motions are better known. This will require observations with high spatial and temporal resolution as well as dynamical models of the phenomena in question. Meanwhile, we regard microturbulence and macroturbulence as fitting parameters. Since we recognize that anisotropy is an essential element in all observed components, we do admit anisotropy in our computations, simply by entering the rms average of the assumed vertical and horizontal microturbulence components in the CRD and PRD radiative transfer computations, and in the profile synthesis the usual squared sum of the line-of-sight projections of the vertical and horizontal components of the microturbulence and the macroturbulence.

III. RESULTS

a) Parameter Values

We have done a limited amount of profile fitting, largely concentrating on the $\mu = 1$ and $\mu = 0.16$ profiles of λ5854, because the total source function for this line is largely without PRD effects, and is therefore less sensitive to the microturbulence than the λ4554 line. We fitted the outer wings by adjusting the barium abundance. Their center-limb variation permits the separation of the effects of the abundance and of the collisional damping; the Deridder–Van Rensbergen damping value is satisfactory, and the barium abundance is $A_{Ba} = 1.9 \times 10^{-10} A_H$. We use the inner wings and core of λ5854 to derive the microturbulence. Starting with the Canfield-Beckers (1976) reference model, we arrived at the model of Table 1, which is piecewise linear between the tabulated values

TABLE 1

TURBULENCE MODEL

HEIGHT (km)		MICROTURBULENCE		
HSRA Scale	Eclipse Scale	Vertical	Horizontal	rms
−54	−391	1.8	3.2	2.6
+25	−312	1.8	2.4	2.1
+206	−131	0.3	0.8	0.6
+335	−2	0.3	0.8	0.6
+454	+118	0.3	1.5	1.1
+478	+141	0.3	1.5	1.1
+747	+410	1.5	1.5	1.5
+1707	+1370	1.5	1.5	1.5

Macroturbulence (km s^{-1}):
Vertical, 1.3
Horizontal, 2.0

of the vertical and horizontal components. This model does not contain the steep outward rise of the Canfield-Beckers model for the total (micro + macro) turbulence. Such a rise in the microturbulence would bring so many wing photons into the λ4554 core that its source function would rise and produce emission cores near the limb that are not observed.

Finally, the macroturbulence is set by fitting the observed λ5854 line center intensities at $\mu = 1$ and $\mu = 0.16$ (Table 1).

b) The λ4554 Resonance Line

The source function of λ4554 in both the PRD and CRD cases is shown in Figure 1. The line source function (left) indeed displays the "fishbone" structure with frequency derived empirically in Paper I; it follows $J_\nu(h)$ outward in the wings from the height where $\lambda_{Coll} \approx \gamma_{Rad}$. The precise pattern is set by γ_{Coll} and the microturbulence. For larger γ_{Coll} the dip in the wing source functions near $h = -60$ km deepens; the microturbulence affects especially the inner wing source function near $\Delta\lambda = 0.06$ Å.

The line is strong enough that some of this frequency-dependence shows in the total source function (Fig. 1, right) even below the temperature minimum. The resulting disk and limb profiles are compared to the observations in Figures 2 and 3. The disk profiles fit well in the outer wings, showing that γ_{Coll} and the abundance are approximately correct. However, their cores are too deep, a fault shared by all our calculations. To remedy this, the line center source function has to be higher at the surface. The macroturbulence cannot be increased because then the boxy, observed, hyperfine structure pattern of the core would be obliterated. We expect that extending the model atom, especially with the λ4934 resonance line, would indeed raise the surface value of the λ4554 core source function by providing more paths to the upper level. This is the case for Ca II (Shine *et al.* 1975, Table Ib), and this example indicates also that the λ4554 wings and the λ5854 line will not change much when the model is extended.

The differences between the PRD and CRD profiles are small on the center of the disk (1% of the

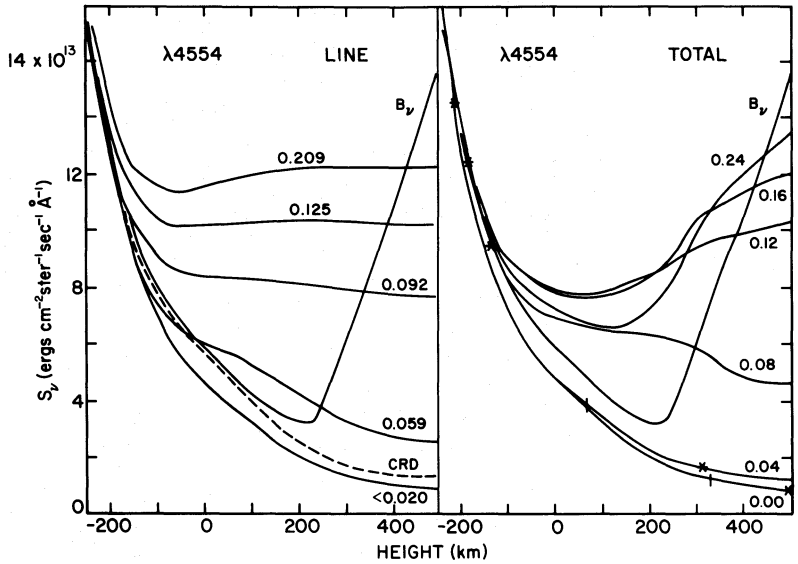

FIG. 1.—Source function of Ba II λ4554. *Left*, CRD and PRD line source functions. The various PRD components are indicated by their wavelength separation from line center in Å. *Right*, total PRD source function (continuum + line, including line hyperfine structure). The heights where $\tau_\nu = 1$, measured along the line of sight, are indicated: ticks at $\Delta\lambda = 0$ and $\Delta\lambda = 0.04$ Å are for disk center, asterisks at $\Delta\lambda = 0$, 0.04, 0.08, 0.12 and 0.16 Å are for $\mu = 0.16$ (where $\mu = \cos\theta$, with θ the viewing angle between the line of sight and the radius vector).

continuous intensity in the core), but increase toward the limb (4% in the wings) where the frequency-dependent wing source structure becomes noticeable.

The computed extreme limb profiles (Fig. 3) are quite different for PRD and for CRD. They confirm the conclusion of Paper I that the PRD source function explains the observed wing emission inside the limb.

The computed emission wings do not depend strongly on the microturbulence; they are similar in all our PRD computations. The cores of the limb profiles are deeper than observed, again indicating a larger surface value for the λ5544 core source function.

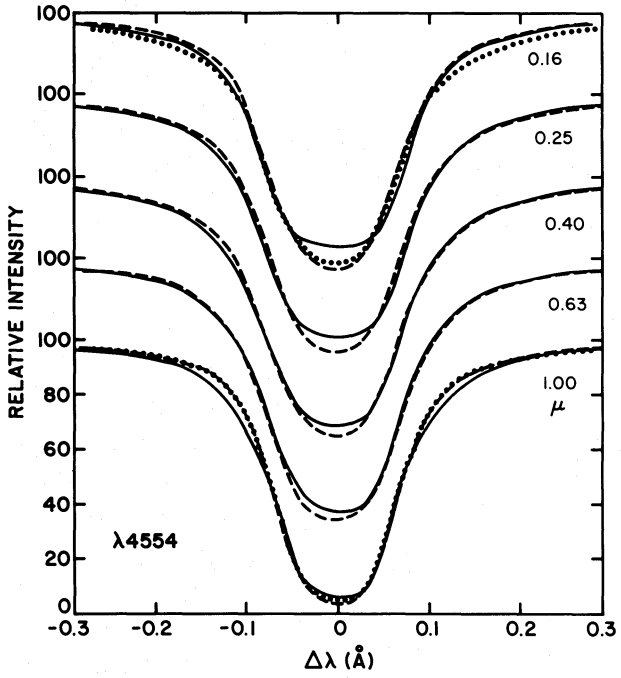

FIG. 2.—Center-to-limb variation of the λ4554 line. Observed profiles (*solid lines*) and computed profiles, scaled to the continuum intensity (=100%), for the various viewing angles indicated. Vertical offsets are 30%. *Dashed lines*, PRD profiles; *dotted lines*, CRD profiles ($\mu = 1$ and $\mu = 0.16$ only).

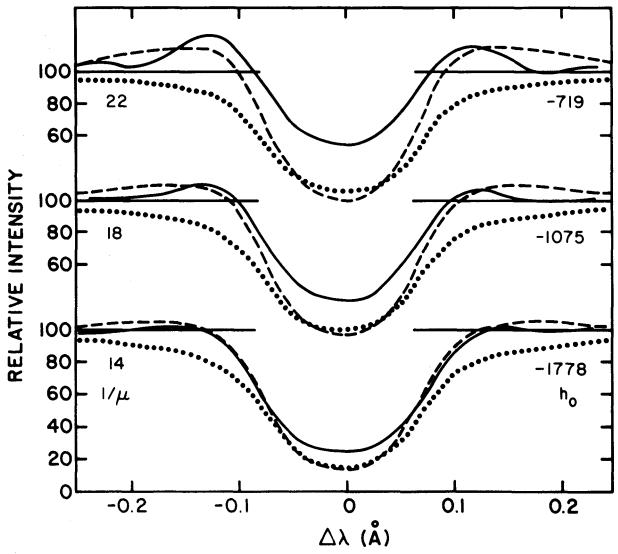

FIG. 3.—Extreme limb profiles for λ4554. Observed profiles (*lines*) and computed profiles, scaled to the continuum (=100%), for the lunar limb positions indicated. The heights h_0 specify the distance of the Moon's limb from the solar limb, in km. Vertical offsets are 80%. *Dashed lines*, PRD profiles; *dotted line*, CRD profiles.

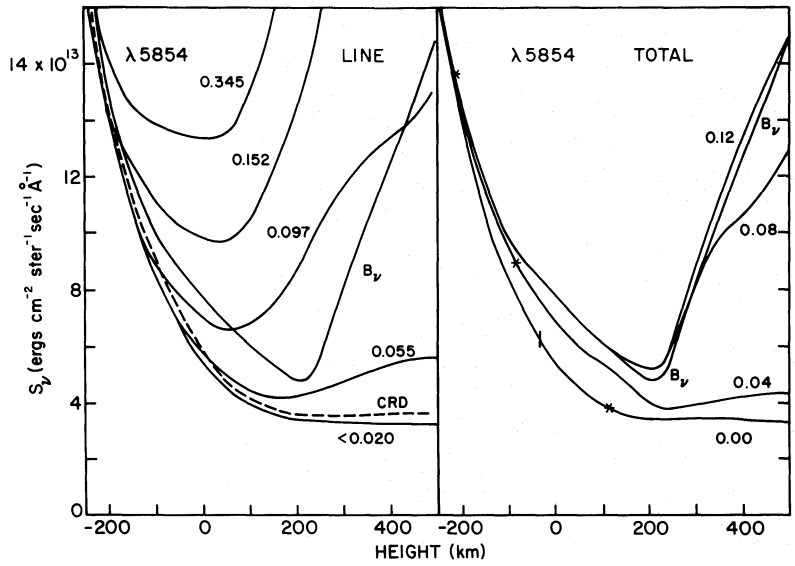

FIG. 4.—Source function of Ba II λ5854. *Left*, CRD and PRD line source functions. Labeling as in Fig. 1. *Right*, total PRD source function. Labeling as in Fig. 1. Heights with $\tau_\nu = 1$ are indicated at $\Delta\lambda = 0.0$ Å at disk center (*tick*) and at $\Delta\lambda = 0$, 0.04 Å and ≥ 0.08 Å for $\mu = 0.16$ (*asterisks*).

Profiles for lines of sight toward the limb proper ($h_0 = 0$) and above it were also computed. They are similar to those in Paper I; they agree well with the observed profile shapes in the case of PRD, and not at all in the case of CRD.

c) *The λ5854 Subordinate Line*

The source function of λ5854 is shown in Figure 4. While the PRD line source function shows a strong dependence on frequency above $h = -200$ km, the total source function is quite similar to the CRD source function. This line is so weak that CRD is an acceptable approximation even at the limb. However, its departure from LTE is large: the line source function falls below B_ν quite deep in the photosphere, owing to photon loss to the resonance line. Our computations for λ6142 show a similar behavior.

The predicted profiles are compared to the observations in Figure 5. The PRD and CRD profiles are identical except in the line core, where the PRD profiles are deeper by 1% of the continuous intensity.

Holweger and Müller (1974), in their analysis of the solar Ba II spectrum, used an LTE model with an outwardly decreasing temperature that is approximately 150 K hotter than the HSRA at the height of the latter's minimum, inevitably leading to a much too shallow line core for the λ5854 line. They noted this discrepancy as an indication that non-LTE affects only the line core. In Figure 5, we extend their model toward the limb. The wings become far too deep, showing that their method of increasing γ_{Coll} to fit all disk-center equivalent widths with a single abundance value and an LTE model leads to an unsatisfactory representation of the wings near the limb as well.

Profiles of λ5854 were also computed at the extreme

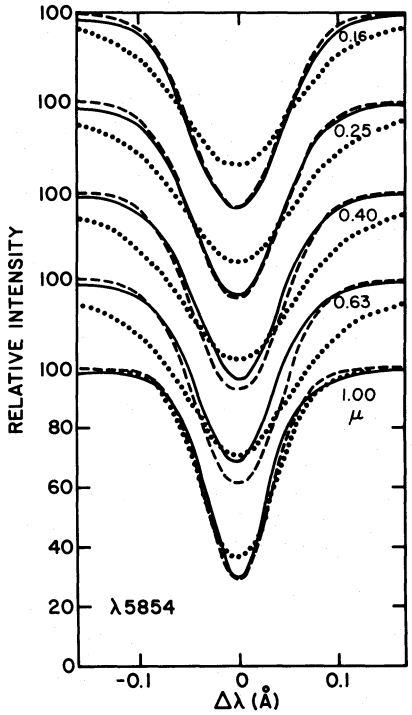

FIG. 5.—Center-to-limb variation of the λ5854 line. Labeling as for Fig. 2. *Solid lines*, observed profiles; *dashed lines*, computed PRD profiles; *dotted lines*, computed LTE Holweger-Müller profiles (atmospheric model, abundance, damping, macroturbulence and vertical microturbulence taken from Holweger and Müller 1974; horizontal microturbulence from Garz *et al.* 1969).

limb. From the source function (Fig. 4) one would expect emission only for $h_0 > 0$, where the continuum optical depth along the line of sight is less than unity, and at most a weak reversal at $h_0 = 0$, with weakened wing emission because the line source function drops below B_ν at $h = 0$. The computations show an absorption profile for $h_0 < 0$, a slight reversal at $h_0 = 0$, and a simple emission line above the limb. This prediction can be compared qualitatively to observations, since Livingston and White (1974) have published a limb spectrogram, taken during very good seeing, which contains λ5854. We simulate their observation by integrating our computed profiles over their projected slit width (340 km) for various assumed positions of the slit. The results show a reversal for slit center positions between $h_0 = 0$ and 100 km. Inside the limb, the predicted profile is a normal absorption line. Inspection of the original spectrogram shows that these computations are in good qualitative agreement with the observations. Livingston and White estimated that the center of their tangentially placed slit was located at $h_0 = -130$ km, and the spectrogram indeed shows no emission at that location. Farther outward, along the slit, it shows a reversal with the faint absorption core rapidly disappearing. While the emission in the reversal exhibits fine structure knots of $\approx 1''$ size, these are superposed on a homogeneous reserval pattern. The latter is adequately mimicked by our one-dimensional calculation.

V. CONCLUSIONS

Our non–LTE line formation computations confirm the empirical result of Paper I that effects of partial redistribution are present in the formation of Ba II λ4554, and that these effects cause the emission wings which this photospheric line displays near the solar limb. This emission can therefore be explained without invoking effects of inhomogeneities; also the slight reversal exhibited by the weak CRD λ5854 line at the limb itself is compatible with the one-dimensional prediction.

However, a better understanding of inhomogeneities and nonthermal velocity fields and their effects on spatially unresolved line profiles will probably lead to quantitative changes in our model, especially for the λ4554 line, since its frequency redistribution is strongly influenced by the amount and nature of the nonthermal motions. We note that if, as we suspect, some of the so-called "microturbulence" is due to large-scale motions, the degree of coherency will be even larger than derived here.

A comparison with the previous Ba II studies illustrates the uniqueness problem in stellar spectroscopy. In Paper I (Rutten 1978), a maximum number of observational constraints were employed in the analysis of λ4554. The derived empirical model agrees with the theoretical results of the present analysis, including the PRD effects. On the other hand, the weak λ5854 line, for which fewer observational constraints were available (no limb data), is now found to deviate appreciably more from LTE than was found in the empirical study. Finally, the minimum-constraint abundance analysis of Holweger and Müller (1974), based on disk-center data only, employs a model for Ba II line formation which is clearly too simplified for anything other than an abundance analysis. Our result for the barium abundance ($A_{\rm Ba} = 1.9 \times 10^{-10} A_{\rm H}$) does not differ greatly from theirs ($A_{\rm Ba} = 1.3 \times 10^{-10} A_{\rm H}$), although it does lie outside their quoted error range, and it is closer to the meteoritic value ($A = 2.1 \times 10^{-10}$ for the Orgueil meteorite; see Holweger and Müller 1974).

A direct observational proof of the presence of coherent scattering in the λ4554 line is the recent observation by Wiehr (1978) of its linear polarization near the limb; the presence of line polarization has been confirmed even more recently by Stenflo (private communication).

We expect that the λ4554 limb emission wings mimic the weak Ca II limb emission lines in showing only slight spatial fine structure (see Canfield and Stencel 1976), because their formation by coherently scattered radiation from deep photospheric layers implies extensive spatial averaging. Also, the far wings of Ca II H and K should display a similar fish-bone source function structure, which may become noticeable toward the limb.

We are indebted to Dr. L. E. Cram for diagnosing a programming error and for many comments on the paper, and to Dr. W. C. Livingston for showing us the λ5854 limb spectrogram. R. J. R. thanks the director, Dr. J. B. Zirker, and the staff of the Sacramento Peak Observatory for their hospitality. The NATO Fellowship he held there was awarded by the Netherlands Organization for the Advancement of Pure Research (ZWO). The Utrecht 1970 eclipse expedition which obtained the λ4554 limb spectrograms was also funded by ZWO. The disk observations were obtained by Dr. H. Nieuwenhuijzen and L. Testerman at Kitt Peak National Observatory.

REFERENCES

Canfield, R. C. 1969, *Ap. J.*, **137**, 425.
———. 1971, *Astr. Ap.*, **10**, 64.
Canfield, R. C., and Beckers, J. M. 1976, in *Physique des mouvements dans les atmosphères stellaires*, ed. R. Cayrel and M. Steinberg, Colloques Internationaux du CNRS No. 250.
Canfield, R. C., and Cram, L. E. 1977, *Ap. J.*, **216**, 654.
Canfield, R. C., and Stencel, R. E. 1976, *Ap. J.*, **209**, 618.
Deridder, Gh., and Van Rensbergen, W. 1974, *Solar Phys.*, **34**, 77.
Fullerton, W., and Cowley, Ch. R. 1971, *Ap. J.*, **165**, 643.
Garz, T., Holweger, H., Keck, M., and Richter, J. 1969, *Astr. Ap.*, **2**, 466.
Gingerich, O., Noyes, R. W., Kalkofen, W., and Cuny, Y. 1971, *Solar Phys.*, **18**, 347.
Holweger, H., and Müller, E. A. 1974, *Solar Phys.*, **39**, 19.
Keil, S. L., and Canfield, R. C. 1978, *Astr. Ap.*, **70**, 169.
Livingston, W. C., and White, O. R. 1974, *Solar Phys.*, **39**, 289.
Magnan, C. 1975, *J. Quant. Spectrosc. Radiat. Transfer*, **15**, 979.

Milkey, R. W. 1976, in *Interpretation of Atmospheric Structure in the Presence of Inhomogeneities*, ed. C. J. Cannon, University of Sydney Printing Office.
Milkey, R. W., and Mihalas, D. 1973*a*, *Ap. J.*, **185**, 709.
———. 1973*b*, *Solar Phys.*, **32**, 361.
———. 1974, *Ap. J.*, **192**, 769.
Milkey, R. W., Shine, R. A., and Mihalas, D. 1975, *Ap. J.*, **199**, 718.
Rutten, R. J. 1977, *Solar Phys.*, **51**, 3.
———. 1978, *Solar Phys.*, **56**, 237 (Paper I).
Shine, R. A., Milkey, R. W., and Mihalas, D. 1975, *Ap. J.*, **199**, 724.
Tandberg-Hanssen, E. 1964, *Ap. J. Suppl.*, **9**, 207.
Tandberg-Hanssen, E., and Smythe, C. 1970, *Ap. J.*, **161**, 289.
Thomas, R. N. 1957, *Ap. J.*, **125**, 260.
Underhill, A. B. 1973, in *Stellar Chromospheres*, ed. S. D. Jordan and E. H. Avrett, NASA Special Publication 317, p. 56.
Vardavas, I. M., and Cram, L. E. 1974, *Solar Phys.*, **38**, 367.
Vernazza, J. E., Avrett, E. H., and Loeser, R. 1973, *Ap. J.*, **184**, 605.
Wiehr, E. 1978, *Astr. Ap.*, **67**, 257.

ROBERT W. MILKEY: Kitt Peak National Observatory, 950 North Cherry Avenue, P.O. Box 26732, Tucson, AZ 85726

ROBERT J. RUTTEN: Sterrekundig Institute te Utrecht, Zonnenburg 2, Utrecht, Holland